

Supplementary Information (SI)

Transition Pathways Towards Net-Zero Emissions Methanol Production

Muflih A. Adnan^{1,2,+}, M.A. Khan^{1,+}, Pulickel M. Ajayan³, Muhammad M. Rahman³, Jinguang Hu,^{1, *} and Md Golam Kibria^{1, *}

⁺Equal contribution

¹Department of Chemical and Petroleum Engineering, University of Calgary, 2500 University Drive, NW, Calgary, Alberta T2N 1N4, Canada.

²Department of Chemical Engineering, Islamic University of Indonesia, Sleman, Daerah Istimewa Yogyakarta, 55584, Indonesia

³Department of Materials Science and NanoEngineering, Rice University, 6100 Main St., Houston, TX 77030, USA.

*Correspondence: jinguang.hu@ucalgary.ca; md.kibria@ucalgary.ca

1. Process parameters

An emerging Direct Air Capture (DAC) technology is being developed by wide spectrum of communities as reflected by several companies that have focused on commercialization of DAC process (Table S.1). Simultaneously, the studies on power-to-methanol routes significantly grow as presented in Table S.2. Few of them are planned for deployment as a pilot-scale power-to-methanol (Table S.3). A Proton Exchange Membrane (PEM) electrolyzer is used to facilitate H₂O electrolysis in 1st generation, while an alkaline electrolyzer is selected to facilitate CO₂ electrolysis in 2nd generation, Aspen Plus is used to model the CO₂ hydrogenation reactions, gas-liquid separation, compression, and distillation (Table S.4). Detail description of simulation is available in Section 3 of the Supplementary Information. In the hydrogenation reactor, the kinetic parameters are adapted from the Haldor Topsøe MK 101 catalysts¹. Under similar conditions (adiabatic reactor) and feed compositions (H₂ (79.8%), CO (11.4%) and CO₂ (8.8%) at 523.4 K and 30 bar), the model of hydrogenation reaction in this study is in good agreement with the one reported in the literature ². The Soave-Redlich-Kwong (SRK) equation of state is selected as a thermodynamic package in the Aspen Plus simulation given it provides high accuracy in the MeOH production process, as reported in the literature ³⁻⁶. To accommodate liquid-liquid separation for MeOH purification, the Non-Random Two-Liquid (NRTL)-RK is selected in the distillation unit. The capital and operating costs of the Aspen Plus-simulated processes is estimated using Aspen Process Economic Analyzer.

Table S.1 List of companies working to commercialize Direct Air Capture technology.

| No. | Company | Capturing agent/process | Capacity | Ref. |
|-----|--------------------|-------------------------|-------------------|------|
| 1 | Carbon Engineering | KOH/CaCO ₃ | 1 ton per day | 7, 8 |
| 2 | Climeworks | Amine | 1000 ton per year | 8, 9 |
| 3 | Global Thermostat | Amine | 1000 ton per year | 8 |
| 4 | Infinitree | Ion-exchange | Lab-scale | 8 |
| 5 | Skytree | Benzylamines | Appliance | 8 |

Table S.2 List of literature on techno-economic and life cycle analysis on power to methanol synthesis.

| No. | Process | MeOH price (\$/ton MeOH) | Remarks | Ref. |
|-----|-----------------------------------------------------------------|--------------------------|-------------------------------------------------------------------------------------------------------------------------------------------------------------------------------------|---------------|
| 1 | H ₂ O electrolysis and CO ₂ hydrogenation | 670 | -Electricity cost = \$0.048/kWh -Natural gas cost = 6 US\$/GJ -CO ₂ cost (post-combustion) = 18 US\$/ton CO ₂ -Life cycle assessment is not reported | ¹⁰ |
| 2 | H ₂ O electrolysis and CO ₂ hydrogenation | 725 | -Electricity cost = \$0.048/kWh -CO ₂ source is post-combustion CO ₂ capture -Life cycle assessment is not reported | ¹¹ |
| 3 | H ₂ O electrolysis and CO ₂ | 970 | -Electricity and CO ₂ are supplied by wind turbine and direct air capture, | ¹² |

| | | | | |
|---|-----------------------------------------------------------------------------------------|------------------------------------------|----------------------------------------------------------------------------------------------------------------------------------------------------------------------------------------------------------------------------------------------------------------|----|
| | hydrogenation | | respectively -Life cycle assessment is not reported | |
| 4 | H ₂ O electrolysis and CO ₂ hydrogenation | 735 – 1955 (grid) 1155 (onshore wind) | -Electricity (grid) cost: 0.045 – 0.162 \$/kWh -Electricity (onshore wind) cost: \$0.050/kWh -CO ₂ is captured from ammonia or biogas process emission -Cradle-to-gate CO ₂ emission (net) = – 868 kg-CO ₂ /ton-MeOH | 13 |
| 5 | H ₂ O electrolysis and CO ₂ hydrogenation | 1,105 | -Electricity (grid) cost: \$0.05/kWh -CO ₂ cost (post-combustion) = \$53/ton CO ₂ -Life cycle assessment is not reported | 14 |
| 6 | Direct CO ₂ -to-methanol electrolysis | 1600 | -CO ₂ cost = \$60/ton CO ₂ -Electricity cost = \$0.04/kWh -Cradle-to-gate CO ₂ emission (net) = 512 kg-CO ₂ /ton-MeOH | 15 |
| 7 | H ₂ O electrolysis and CO ₂ hydrogenation | 850 | -CO ₂ cost = \$60/ton CO ₂ -Electricity cost = \$0.04/kWh -Cradle-to-gate CO ₂ emission (net) = 558 kg-CO ₂ /ton-MeOH | 15 |
| 8 | H ₂ O electrolysis, CO ₂ -to-CO electrolysis and CO hydrogenation | 1000 | -CO ₂ cost = \$60/ton CO ₂ -Electricity cost = \$0.04/kWh -Cradle-to-gate CO ₂ emission (net) = 470 kg-CO ₂ /ton-MeOH | 15 |

Table S.3 Pilot-scale power to methanol

| No. | Company | Process | Methanol production | Ref. |
|-----|-----------------------------------------------------------------------------------------------------------|-----------------------------------------------------------------|-------------------------------------------------------|------|
| 1 | MefCO ₂ consortium | H ₂ O electrolyzer and CO ₂ hydrogenation | 1 ton per day | 16 |
| 2 | Carbon Recycling International (CRI) | H ₂ O electrolyzer and CO ₂ hydrogenation | 4000 ton per year | 17 |
| 3 | Consortium (Engie, Fluxys, Indaver, Inovyn, Oiltanking, Port of Antwerp and the PMV (Flemish Government)) | Undisclosed | 8000 ton per year (scheduled start in 2022) | 18 |
| 4 | Shunli and Carbon Recycling International | Undisclosed | 110,000 ton per year (scheduled start by end of 2021) | 19 |

Table S.4 Summary of the key parameters of air-to-MeOH routes

| Description | 1 st generation (Two-step air-to-MeOH) | 2 nd generation (Single-step air-to-MeOH) |
|-------------|------------------------------------------------------|---------------------------------------------------------|
| Main feeds | CO ₂ H ₂ O | CO ₂ H ₂ O |

Preparation

| | | |
|----------------------|-------------------------------|----------------|
| Equipment | H ₂ O electrolyzer | Not applicable |
| Reaction | R1 | Not applicable |
| Aspen Plus | External ¹⁾ | Not applicable |
| Operating Conditions | See Table 2 | Not applicable |
| Utilities | Electricity | Not applicable |

MeOH synthesis

| | | |
|----------------------|-------------------------------|------------------------------|
| Equipment | CO ₂ hydrogenation | CO ₂ electrolyzer |
| Reaction | R2, R3, R4 | R6 |
| Aspen Plus | RPLUG ²⁾ | External ¹⁾ |
| Operating Conditions | See Table S.5 | See Table 2 |
| Utilities | Natural gas | Electricity |

Product purification

| | | |
|--------------------|-------------------------------|-------------------------------|
| Equipment | Distillation | Distillation |
| Aspen Plus | RadFrac ⁴⁾ | RadFrac ³⁾ |
| Utilities | Natural gas Cooling water | Natural gas Cooling water |
| Energy consumption | ~38 GJ/ton MeOH ²⁰ | ~60 GJ/ton MeOH ²¹ |

¹⁾ Please refer to Section 2 for the detail description of external calculation

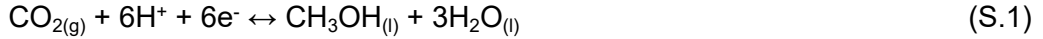
²⁾ Please refer to Section 3 for the kinetic parameters of hydrogenation reaction

³⁾ Total condenser

⁴⁾ Partial vapor-liquid condenser

2. Electrochemical reaction

We select the CO₂ electrolysis for methanol production as an example. We specified the production rate of 46,481 kg methanol/hour is produced by the CO₂ electrolysis with the faradaic efficiency of 90%. With the molecular weight of methanol of 32 kg/kmol, the flowrate of methanol production is 403.5 mol/s. The Faraday constants is 96,480 C/s. Based on the reaction of electroreduction of CO₂ into methanol (S.1), we note that the number of required electrons for completing the reaction is 6 electrons.



Thus, the required current (I) can be estimated as follow:

$$I = \frac{(6)(96,480 \text{ C/s})(403.5 \text{ mol/s})}{(90\%)} \quad (\text{S.2})$$

$$I = 259,521,010 \text{ A} \quad (\text{S.3})$$

Based the calculated current density in Eq. (S.3), we estimate the mass balance of the electrolyzer.

The required flowrate of CO₂ in the cathode side can be estimated by Eq. (S.4).

$$F_{\text{CO}_2} = \frac{(259,521,010 \text{ A})(90\%)}{(6)(96,480 \text{ C/s})} = 403.5 \frac{\text{mol}}{\text{s}} = 63,912 \frac{\text{kg}}{\text{h}} \quad (\text{S.4})$$

Considering the CO₂ conversion of 50%, the CO₂ flowrate entering the electrolyzer is calculated in Eq. (S.5).

$$F_{\text{CO}_2, \text{in}} = \frac{63,912 \frac{\text{kg}}{\text{h}}}{50\%} = 127,823 \frac{\text{kg}}{\text{h}} \quad (\text{S.5})$$

Thus, the CO₂ outlet stream of the electrolyzer is calculated as follow:

$$F_{\text{CO}_2, \text{out}} = \left(127,823 \frac{\text{kg}}{\text{h}}\right)(50\%) = 63,912 \frac{\text{kg}}{\text{h}} \quad (\text{S.6})$$

Please note that the faradaic efficiency of the electrolyzer in 90%. This indicates that 10% of electrons promotes H₂ formation. The flowrate of H₂ is calculated in Eq. (S.7).

$$F_{\text{H}_2, \text{out}} = \frac{(259,521,010 \text{ A})(10\%)}{(6)(96,480 \text{ C/s})} = 134 \frac{\text{mol}}{\text{s}} = 968 \frac{\text{kg}}{\text{h}} \quad (\text{S.7})$$

Besides H₂, H₂O is also produced in the cathode side Eq. (S.8).

$$F_{\text{H}_2\text{O}, \text{out}} = \frac{(259,521,010 \text{ A})(90\%)}{(6)(96,480 \text{ C/s})} = 403.5 \frac{\text{mol}}{\text{s}} = 26,146 \frac{\text{kg}}{\text{h}} \quad (\text{S.8})$$

The flowrate of H₂O enters the anode side is calculated as follows:

$$F_{\text{H}_2\text{O}} = \frac{(259,521,010 \text{ A})(100\%)}{(2)(96,480 \text{ C/s})} = 1,345 \frac{\text{mol}}{\text{s}} = 87,156 \frac{\text{kg}}{\text{h}} \quad (\text{S.9})$$

The flowrate of O₂ product from the anode side is calculated as follow:

$$F_{O_2} = \frac{(259,521,010 \text{ A})(100\%)}{(4)(96,480 \text{ C/s})} = 672 \frac{\text{mol}}{\text{s}} = 77,469 \frac{\text{kg}}{\text{h}} \quad (\text{S.10})$$

3. Process Simulation

3.1. Hydrogenation reaction

The hydrogenation reactor is simulated in the Aspen Plus as RPlug with the specification as mentioned in Table S.5.

Table S.5 Operating conditions for the hydrogenation reactor

| Operating conditions | Values |
|-----------------------------------------------------------|-------------------------------------------------------|
| Temperature (K) | 323 – 511 |
| Pressure (bar) | 69 (in) – 67 (out) |
| Length (cm) | 1200 |
| Number of tubes | 4650 |
| Tube diameter (cm) | 4.6 |
| Feed specification | $m = (n_{H_2} - n_{CO_2}) / (n_{CO} + n_{CO_2}) = 2$ |
| Conversion | H ₂ = 19%; CO = 82%; CO ₂ = 48% |
| Heating fluid temperature (K) | 511 |
| Thermal conductivity (W m ⁻² K ⁻¹) | 600 W m ⁻² K ⁻¹ |

The kinetic parameters are taken from Graaf et. al.¹. The following reactions occur in the hydrogenation reactor:



Aspen Plus software has standard form for the rate of reaction equation. Thus, one should rearrange the rate equation in Graaf et. al. ¹ to satisfy the Aspen Plus standard. The rearranged rate of reaction equation for reactions Eq. (S.11) to Eq. (S.13) are:

For S.11:

$$r'_{CH_3OH, A3} = \frac{k_A K_{CO} \left(f_{CO} f_{H_2}^{3/2} - \frac{1}{K_{C1}} \frac{f_{CH_3OH}}{f_{H_2}^{1/2}} \right)}{\left(f_{H_2}^{1/2} + \frac{K_{H_2O}}{K_{H_2}^{1/2}} f_{H_2O} + K_{CO} c_{CO} f_{H_2}^{1/2} + \frac{K_{H_2O}}{K_{H_2}^{1/2}} K_{CO} f_{CO} f_{H_2O} + K_{CO_2} f_{CO_2} f_{H_2}^{1/2} + \frac{K_{H_2O}}{K_{H_2}^{1/2}} K_{CO_2} f_{CO_2} f_{H_2O} \right)}$$

For S.12:

$$r'_{CH_3OH, B2} = \frac{k_B K_{CO_2} \left(f_{CO_2} f_{H_2} - \frac{1}{K_{C2}} f_{H_2O} f_{CO} \right)}{\left(f_{H_2}^{1/2} + \frac{K_{H_2O}}{K_{H_2}^{1/2}} f_{H_2O} + K_{CO} f_{CO} f_{H_2}^{1/2} + \frac{K_{H_2O}}{K_{H_2}^{1/2}} K_{CO} f_{CO} f_{H_2O} + K_{CO_2} f_{CO_2} f_{H_2}^{1/2} + \frac{K_{H_2O}}{K_{H_2}^{1/2}} K_{CO_2} f_{CO_2} f_{H_2O} \right)}$$

For S.13:

$$r'_{CH_3OH, C3} = \frac{k_C K_{CO_2} \left(f_{CO_2} f_{H_2}^{3/2} - \frac{1}{K_{C3}} \frac{f_{CH_3OH} f_{H_2O}}{f_{H_2}^{3/2}} \right)}{\left(f_{H_2}^{1/2} + \frac{K_{H_2O}}{K_{H_2}^{1/2}} f_{H_2O} + K_{CO} f_{CO} f_{H_2}^{1/2} + \frac{K_{H_2O}}{K_{H_2}^{1/2}} K_{CO} f_{CO} f_{H_2O} + K_{CO_2} f_{CO_2} f_{H_2}^{1/2} + \frac{K_{H_2O}}{K_{H_2}^{1/2}} K_{CO_2} f_{CO_2} f_{H_2O} \right)}$$

The values in the following tables is used in the Aspen Plus for determining the kinetic parameter of hydrogenation reaction (RPLUG).

Table S.6 The value of kinetic factor

| Reaction | k, kmol/(s kg) | E, kJ/kmol |
|----------|-----------------------|------------|
| S.11 | 4.89×10^{-1} | -113000 |
| S.12 | 3048426 | -152900 |
| S.13 | 0.00109 | -87500 |

Table S.7 The value of driving force

| Reaction | Term-1 | | Term-2 | |
|----------|--------|------|--------|-------|
| | A | B | A | B |
| S.11 | -22.26 | 5629 | 29.83 | -6204 |
| S.12 | -25.68 | 7421 | -30.35 | 12194 |
| S.13 | -25.68 | 7421 | 21.74 | 361 |

Table S.8 The value of adsorption constant

| Term no. | 1 | 2 | 3 | 4 | 5 | 6 |
|---------------|---|--------|--------|--------|--------|--------|
| Coefficient A | 0 | -24.63 | -22.26 | -46.88 | -25.68 | -50.31 |
| Coefficient B | 0 | 0 | 0 | 0 | 0 | 0 |

The model in this study is in close agreement with the experiment data under the similar operating conditions, as reported elsewhere ². In this regard, the gas mixture of H₂ (79.8%), CO (11.4%) and CO₂ (8.8%) was directed various ratio of volumetric flow rate to the catalysts weight (ϕ_w/w) to the adiabatic fixed bed reactor (Haldor Topsoe MK 101 catalysts) at 523.4 K and 30 bar. The comparison between our model and the literature ² is presented in Figure S.1.

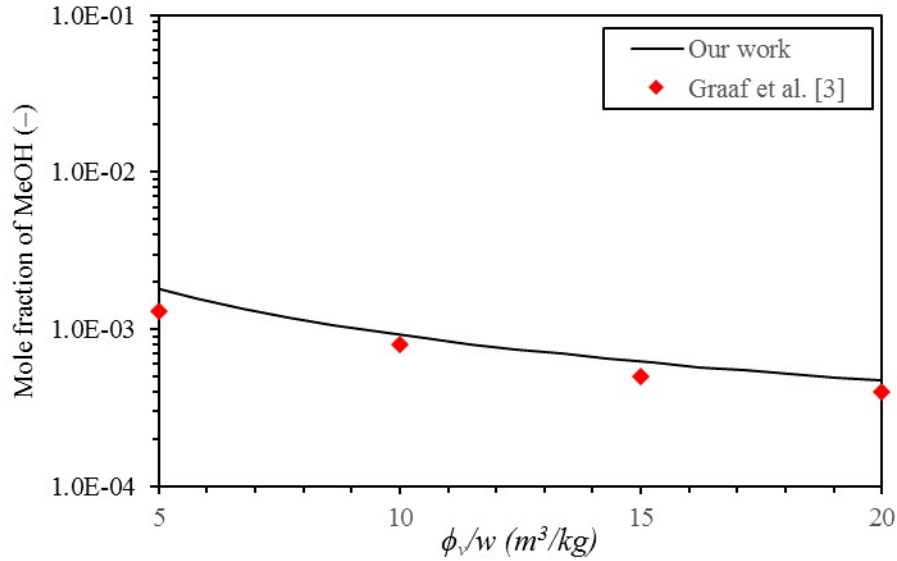


Figure S.1. The mole fraction of methanol in the reactor outlet

3.2. Gas-liquid separation

The mixture of liquid products (MeOH and water) and gas products (CO, CO₂, and H₂) is separated using Flash2 block in Aspen Plus) at 311 K and 67 bars. Under this condition, the gas products are discharged from the top side, while liquid products are dispensed from the bottom side.

3.3. Distillation unit

The liquid products from gas-liquid separation are directed to the distillation unit for product purification. The top and bottom products of distillation unit is MeOH (99 wt.%) and water, respectively. The specification of distillation unit is presented in Table S.9.

Table S.9 The specification of the distillation unit (RadFrac)

| Parameters | Value |
|-----------------------------|----------------------|
| Condenser | Partial-Vapor-Liquid |
| Reboiler | Kettle |
| Valid phases | Vapor-Liquid |
| Reflux ratio | 3.5 |
| Number of stages | 26 |
| Feed stage (from top side) | 20 |
| Condenser temperature | 323.15 K |
| Condenser pressure | 1.01 bar |
| Property method | NRTL-RK |
| Free-water phase properties | STEAMNBS |

3.4. Compressor

Compressors are important to increase the stream pressure given the hydrogenation reactor operate at elevated pressure. Compressor is simulated using Compr block with the typical specification as listed in Table S.10.

Table S.10 The specification of the compressors (Compr)

| Parameters | Value |
|-----------------------|------------------------------|
| Type | Polytropic using ASME method |
| Polytropic efficiency | 85% |
| Mechanical efficiency | 99% |
| Compression ratio | 3 |

4. Mass balance

The mass balances of the studied air-to-methanol routes are presented in Figure S.2 and Figure S.3.

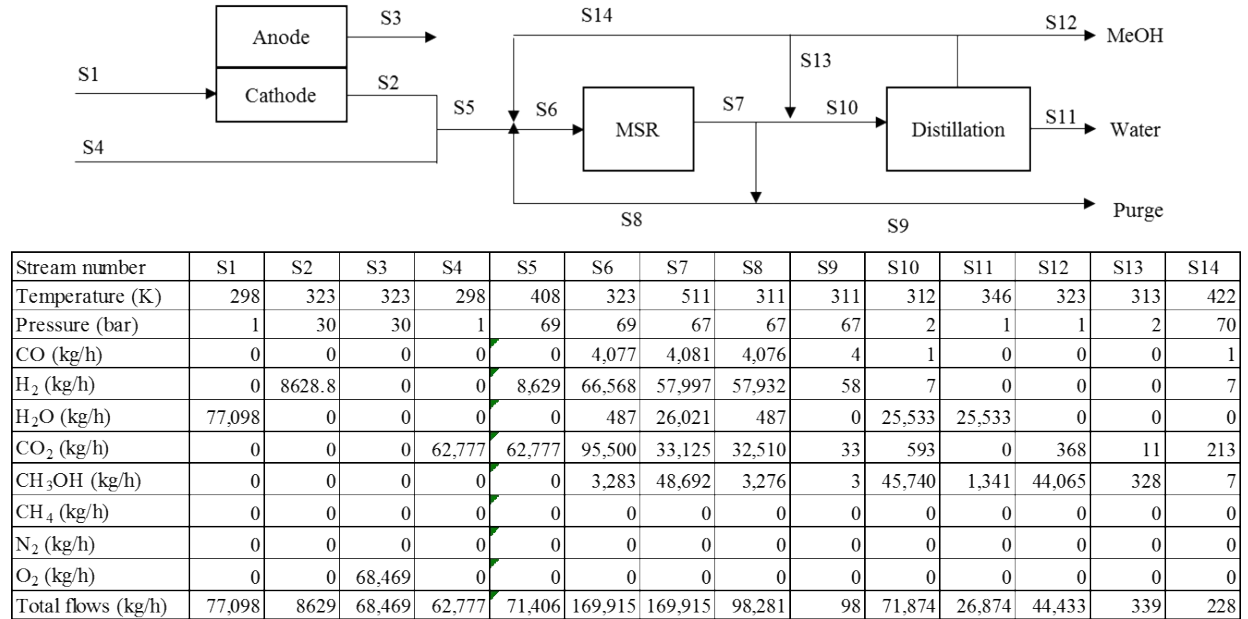
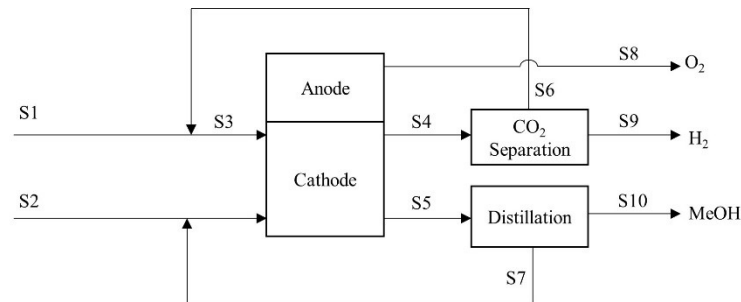


Figure S.2 The mass balance of 1st generation (please note that pressure and heat changers may exist between streams)



| Stream number | S1 | S2 | S3 | S4 | S5 | S6 | S7 | S8 | S9 | S10 |
|---------------------------|--------|--------|---------|--------|--------|--------|--------|--------|-------|--------|
| Temperature (K) | 298 | 298 | 298 | 298 | 298 | 298 | 363 | 323 | 298 | 339 |
| Pressure (bar) | 1 | 1 | 1 | 1 | 1 | 2 | 1 | 180 | 2 | 1 |
| H ₂ (kg/h) | 0 | 0 | 0 | 2,179 | 0 | 0 | 0 | 0 | 2,179 | 0 |
| H ₂ O (kg/h) | 0 | 60,995 | 0 | 0 | 30,988 | 0 | 30,988 | 0 | 0 | 0 |
| CO ₂ (kg/h) | 63,912 | 0 | 127,824 | 63,912 | 0 | 63,912 | 0 | 0 | 0 | 0 |
| CH ₃ OH (kg/h) | 0 | 0 | 0 | 0 | 46,481 | 0 | 11 | 0 | 0 | 46,470 |
| O ₂ (kg/h) | 0 | 0 | 0 | 0 | 0 | 0 | 0 | 77,469 | 0 | 0 |
| Total flows (kg/h) | 63,912 | 60,995 | 127,824 | 66,091 | 77,469 | 63,912 | 30,999 | 77,469 | 2,179 | 46,470 |

Figure S.3 The mass balance of 2nd generation (please note that pressure and heat changers may exist between streams)

5. Economic calculation

The capital cost and operating cost of the Aspen Plus-simulated process such as hydrogenation reactor, distillation, and compression are estimated using Aspen Economic Analyzer. One should note that the capital cost and operating cost covers every single expense in plant construction and operation. In the following texts, we presented the calculation of capital cost and operating cost of electrolyzer, silicon photovoltaic (Si-PV), and direct air capture (DAC).

A. Electrolyzer

In the regard of capital cost of electrolyzer, the CO₂ electrolyzer in 2nd generation is taken as an example. Based on the literature²², the capital cost of alkaline electrolyzer (1 MW system) is 130 \$/kW in the present days, with the reference current density and cell voltage of the given alkaline electrolyzer is 0.3 A/cm² and 2.00 V, respectively. The stack cost of the electrolyzer in \$/kW is converted into \$/m² by considering the reference performance of the alkaline electrolyzer under the given scenario (0.2 A/cm², 1.68 V²²). The optimistic scenario is selected as the example.

Stack cost in power (C_w) = \$130/kW

Current density (I_d) = 0.2 A/cm²

Cell voltage (V_c) = 1.68 V

The stack cost in specific area (C_a) is calculated as follow:

$$\begin{aligned} C_a &= \left(130 \frac{\$}{\text{kW}}\right) \left(\frac{1 \text{ kW}}{1000 \text{ W}}\right) \left(0.2 \frac{\text{A}}{\text{cm}^2}\right) \left(\frac{10^4 \text{ cm}^2}{1 \text{ m}^2}\right) \\ &= 439 \frac{\$}{\text{m}^2} \end{aligned} \quad (\text{S.14})$$

Under the optimistic scenario, the current density of CO₂ electrolyzer is predicted to be 300 mA/cm². The electrolyzer area (A_e) can be calculated as follow:

$$A_e = \frac{259,521,010 \text{ A}}{0.3 \frac{\text{A}}{\text{cm}^2}} = 86,507 \text{ m}^2 \quad (\text{S.15})$$

The total stack cost (C_{ts}) is estimated as follow:

$$\begin{aligned} C_{ts} &= (86,507 \text{ m}^2) \left(439 \frac{\$}{\text{m}^2}\right) \\ &= \$23,253,083 \end{aligned} \quad (\text{S.16})$$

The power required by the electrolysis system is calculated based on the as follow:

$$\begin{aligned} W &= 259,521,010 \text{ A} \times 2 \text{ V} \\ &= 519,042,021 \text{ W} \end{aligned} \quad (\text{S.17})$$

The balance of plant of the electrolyzer (BOP_e) is 43% of the total stack cost. In this regard, the cost in \$/kW is used given the BOPs majorly relates to electrical equipment.

$$\begin{aligned} BOP_e &= (519,042,021 \text{ W})(1 \text{ kW}/1000 \text{ W})(\$60/\text{kW})(43\%) \\ &= \$31,324,641 \end{aligned} \quad (\text{S.18})$$

The installation cost of the electrolyzer (IC_e) is 10% of the total stack cost.

$$\begin{aligned} IC_e &= (\$54,577,724)(10\%) \\ &= \$5,457,772 \end{aligned} \quad (\text{S.19})$$

The total installed cost of CO₂ electrolyzer including BOP (C_{te}):

$$\begin{aligned} C_{te} &= \$23,253,083 + \$31,324,641 + \$5,457,772 \\ &= \$60,035,496 \end{aligned} \quad (\text{S.20})$$

The annual operating and maintenance cost of CO₂ electrolyzer (OM_e) is 2.5% of the total installed cost.

$$\begin{aligned} OM_e &= (\$60,035,496)(2.5\%) \\ &= \$1,500,887/\text{year} \end{aligned} \quad (\text{S.20})$$

B. Silicon photovoltaic (Si-PV)

The 2nd generation route is selected as the example. The capital cost of silicon photovoltaic (Si-PV) is in the optimistic scenario as listed in Table 2.

Required power = 563,900 kW

Module and tracker cost = \$300/kW

Labor, permissiting and installation cost = \$50/kW

Design, permitting and fee = \$50/kW

Total installed Si-PV cost (C_{tpv}) is calculated as follow:

$$\begin{aligned} C_{tpv} &= (300 \text{ \$/kW} + 50 \text{ \$/kW} + 50 \text{ \$/kW}) (563,900 \text{ kW}) \\ &= \$225,560,075 \end{aligned} \quad (\text{S.21})$$

The annual operation and maintenance cost of Si-PV (OM_{pv}) is calculated as follow:

$$OM_{pv} = \left(10.4 \frac{\$}{\text{kW}}\right)(563,900 \text{ kW})$$

$$= \$5,864,562 \quad (\text{S.22})$$

C. Direct air capture (DAC)

The 2nd generation route is selected as the example. The capital cost of DAC in the optimistic scenario (Table 2) is selected for calculation.

CO₂ production capacity = 506,182 ton-CO₂/year

Capital cost = \$174/(ton-CO₂/year)

The total DAC capital cost (C_{dac}) is estimated as follow:

$$C_{dac} = (506,182 \text{ ton-CO}_2/\text{year})(\$174/(\text{ton-CO}_2/\text{year}))$$

$$= \$88,075,698 \quad (\text{S.23})$$

For the electricity consumption, one should note that the DAC is operated with grid electricity for 18 hours (CPV runs for 6 hours).

Natural gas consumption = 2,044,197 GJ/year

Grid electricity consumption = 78,847,608 kWh/year

Operation and maintenance cost excluding electricity and natural gas = \$26/ton-CO₂

Natural gas price = \$4/GJ

Grid electricity price = 3 cents/kWh

The total operating and maintenance cost of DAC (OM_{dac}) is calculated as follow:

$$OM_{dac} = (\$26/\text{ton-CO}_2)(506,182 \text{ ton-CO}_2/\text{year}) + (\$4/\text{GJ})(2,044,197 \text{ GJ}/\text{year})$$

$$+ (3 \text{ cents}/\text{kWh})(78,847,608 \text{ kWh}/\text{year})$$

$$= \$13,160,737/\text{year} + \$8,176,789/\text{year} + \$2,365,428/\text{year}$$

$$= \$23,702,954/\text{year} \quad (\text{S.24})$$

6. CO₂ emissions

The emission factor of grid electricity in various countries is shown in Table S.11. Figure S.4 illustrates the projection of CO₂ emission of methanol production from 1st and 2nd generation routes. Under the optimistic scenario, a grid CO₂ emission of less than ~240 and ~200 kg CO₂/MWh are required to be comparable with the CO₂ emission of the conventional route. The breakdown of emission when the non-intermittent renewables are utilized to substitute the electricity is shown in Figure S.5. The emission factor of renewable electricity is summarized in Table S.12.

Table S.11 The average grid emission in various countries

| Country | Emission factor (kg-CO ₂ /MWh) | Reported year | Reference |
|---------------------|-------------------------------------------|-----------------|-----------|
| Saudi Arabia | 732 | 2019 | 23 |
| India | 708 | 2018 | 23 |
| China | 555 | 2018 | 23 |
| Japan | 506 | 2018 | 23 |
| United States | 453 | 2018 | 23 |
| Russia | 325 | 2019 | 23 |
| European Union (EU) | 242 | 2018 | 24 |
| United states | 241 | Projection 2050 | 25 |
| Canada | 130 | 2018 | 23 |
| European Union (EU) | 87 | Projection 2040 | 24 |
| Sweden | 50 | 2019 | 23 |
| Iceland | 8.3 | 2020 | 26 |

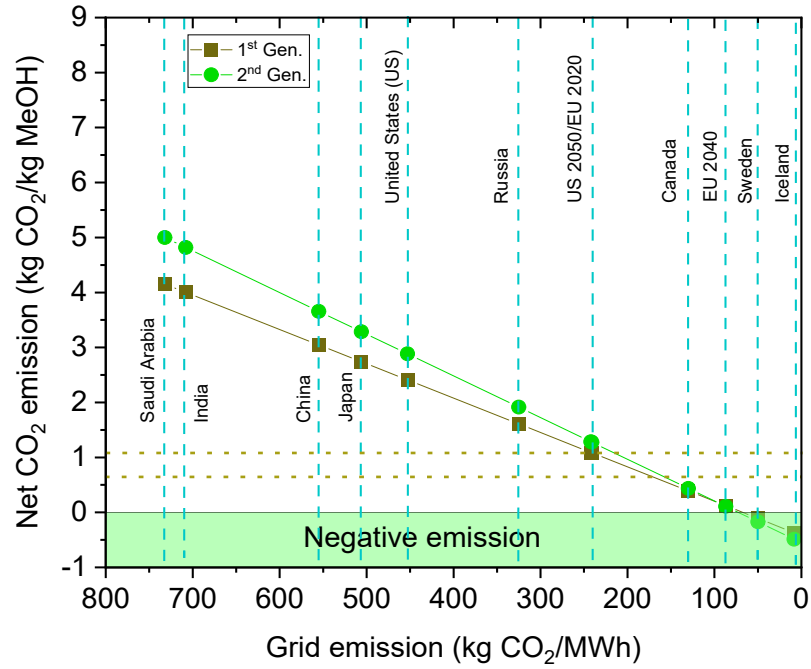


Figure S.4. Net CO₂ emissions from air-to-MeOH production pathways under the optimistic scenario. The blue dashed lines are representative of average electricity emission intensity in various jurisdictions (see Table S.11). The brown dashed lines indicate the range of CO₂ emissions from conventional MeOH synthesis route.²⁷

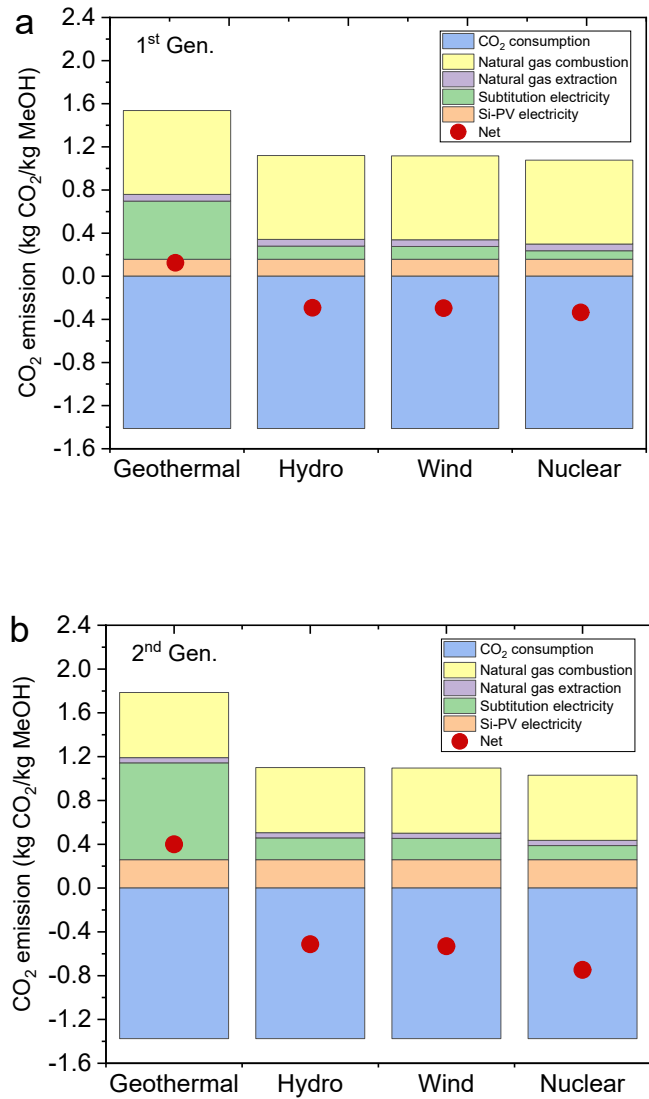


Figure S.5 The breakdown of CO₂ emissions in (a) 1st generation and (b) 2nd generation routes under the base scenario.

Table S.12 The emission factor of renewable electricity

| Electricity source | Emission factor (kg-CO ₂ /MWh) | Reference |
|--------------------|-------------------------------------------|-----------|
| Geothermal | 82 | 28 |
| Hydro | 19 | 29 |
| On shore wind | 18 | 30 |
| Nuclear | 12 | 31 |

References

1. G. H. Graaf, H. Scholtens, E. J. Stamhuis and A. A. C. M. Beenackers, *Chemical Engineering Science*, 1990, **45**, 773-783.
2. G. H. Graaf, J. G. M. Winkelman, E. J. Stamhuis and A. A. C. M. Beenackers, *Chemical Engineering Science*, 1988, **43**, 2161-2168.
3. G. H. Graaf, P. J. J. M. Sijtsema, E. J. Stamhuis and G. E. H. Joosten, *Chemical Engineering Science*, 1986, **41**, 2883-2890.
4. K. M. Vanden Bussche and G. F. Froment, *Journal of Catalysis*, 1996, **161**, 1-10.
5. J. Liu, Z. Qin and J. Wang, *Industrial & Engineering Chemistry Research*, 2001, **40**, 3801-3805.
6. T. Blumberg, G. Tsatsaronis and T. Morosuk, *Fuel*, 2019, **256**, 115824.
7. D. W. Keith, G. Holmes, D. St. Angelo and K. Heidel, *Joule*, 2018, **2**, 1573-1594.
8. E. National Academies of Sciences, and Medicine *Negative Emissions Technologies and Reliable Sequestration: A Research Agenda*, The National Academies Press, Washington, DC, 2019.
9. <https://www.climeworks.com/>, (accessed July 29th, 2020).
10. L. R. Clausen, N. Houbak and B. Elmegaard, *Energy*, 2010, **35**, 2338-2347.
11. C. Bergins, K.-C. Tran, E.-I. Koytsoumpa, E. Kakaras, T. Buddenberg and Ó. Sigurbjörnsson, 2015.
12. M. J. Bos, S. R. A. Kersten and D. W. F. Brilman, *Applied Energy*, 2020, **264**, 114672.
13. C. Hank, S. Gelpke, A. Schnabl, R. J. White, J. Full, N. Wiebe, T. Smolinka, A. Schaadt, H.-M. Henning and C. Hebling, *Sustainable Energy & Fuels*, 2018, **2**, 1244-1261.
14. K. Atsonios, K. D. Panopoulos and E. Kakaras, *International Journal of Hydrogen Energy*, 2016, **41**, 2202-2214.
15. M. A. Adnan and M. G. Kibria, *Applied Energy*, 2020, **278**, 115614.
16. Project Progress, http://www.mefco2.eu/project_progress.php#TOUR, (accessed December 13th, 2020).
17. B. Stefansson, *CO₂-to-methanol: commercial scale technology ready to meet future climate challenges*, Carbon Recycling International.
18. J. Sampson, Consortium established to build 'power-to-methanol' plant, <https://www.gasworld.com/consortium-established-to-build-power-to-methanol-plant/2019069.article>, (accessed April 4th, 2021).
19. M. Burgess, Major milestone reached at "world's first" commercial CO₂-to-methanol plant, <https://www.gasworld.com/major-milestone-achieved-at-co2-to-methanol-plant-in-china/2020547.article>, (accessed April 4th, 2021).
20. W. A. Smith, T. Burdyny, D. A. Vermaas and H. Geerlings, *Joule*, 2019, **3**, 1822-1834.
21. M. Jouny, W. Luc and F. Jiao, *Industrial & Engineering Chemistry Research*, 2018, **57**, 2165-2177.
22. M. Ruth, A. Mayyas and M. Mann, 2017.
23. Country Specific Electricity Grid Greenhouse Gas Emission Factors https://www.carbonfootprint.com/docs/2020_06_emissions_factors_sources_for_2020_electricity_v1_1.pdf.
24. Average CO₂ emissions intensity of hourly electricity supply in the European Union, 2018 and 2040 by scenario and average electricity demand in 2018, <https://www.iea.org/data-and-statistics/charts/average-co2-emissions-intensity-of-hourly-electricity-supply-in-the-european-union-2018-and-2040-by-scenario-and-average-electricity-demand-in-2018>, (accessed October 7th, 2020).
25. Annual Energy Outlook 2020 with projections to 2050, <https://www.eia.gov/outlooks/aeo/pdf/AEO2020%20Full%20Report.pdf>, (accessed September 9th, 2020).

26. Environmental data – Reykjavik Energy 2015-2020, https://annualreport2020.or.is/documents/612/EN_Environmental_data_of_the_OR_Group_2020.pdf, (accessed July 26th, 2021).
27. J. Artz, T. E. Müller, K. Thenert, J. Kleinekorte, R. Meys, A. Sternberg, A. Bardow and W. Leitner, *Chemical Reviews*, 2018, **118**, 434-504.
28. A. Holm, D. Jennejohn and L. Blodgett, *Journal*, 2012.
29. Study shows hydropower’s greenhouse gas footprint, <https://www.hydropower.org/news/study-shows-hydropower%E2%80%99s-carbon-footprint>, (accessed August 29th, 2020).
30. R. C. Thomson and G. P. Harrison, *Journal*, 2015.
31. How can nuclear combat climate change?, <https://www.world-nuclear.org/nuclear-essentials/how-can-nuclear-combat-climate-change.aspx>, (accessed September 16th, 2020).